JOURNAL OF THEORETICAL
AND APPLIED MECHANICS
3, **38**, 2000

NONLINEAR PIEZO-THERMOELASTIC SHELL THEORY APPLIED TO CONTROL OF VARIABLE-GEOMETRY SHELLS

HORN-SEN TZOU

Department of Mechanical Engineering, University of Kentucky, Lexington
e-mail: hstzou@engr.uky.edu

REN JYE YANG

Ford Research Laboratory Vehicle Safety Research Department, Dearborn, USA

Complexity of multi-field opto-thermo-electromechanical coupling always poses many challenging research issues. Recently due to a rapid development in smart structures and structronic systems, multi-field coupling and control of distributed structronic systems also raises variety of new research, development, and system integration issues. This paper presents a generic nonlinear piezo(electric)-thermoelectromechanical shell theory for a piezoelectric double-curvature shell continuum with admissible boundary conditions. Applications of the generic theory to other shell and non-shell continua based on four system parameters are also demonstrated. Detailed sensing and control electromechanical characteristics are further investigated in a series of shells of various curvatures. The results show that the membrane sensing/control component dominates the lower natural modes of deep shells and the bending sensing/control component dominates the natural modes of shallow shells. Electromechanical characteristics and effectiveness of distributed sensors and actuators are evaluated.

Key words: geometric nonlinearity, smart structures, structronics, von Karman nonlinearity

1. Introduction

Recent development of smart structures and structronic systems involves applications of controllable smart materials, e.g., piezoelectrics, shape memory materials, electro- and magneto-strictive materials, electro- and magneto-rheological fluids, etc., to high-performance structures, precision structronic

and mechatronic systems. In general, these smart materials can respond to certain stimuli, e.g., strain, force, pressure, light, etc., and also be actively controlled via electrical field, magnetic field, currents, high-energy lights, etc. (Tzou, 1998). Accordingly, structures and structronic systems incorporating these smart materials are capable of responding to certain stimuli in a prescribed manner based on performance or control requirements (Tzou and Bergamen, 1998). Furthermore, the multi-field coupling and interactions of smart structures and structronic systems have been becoming more and more complicated and deserve an in-depth study to establish profound data base for design of advanced smart structures and structronic systems.

Piezoelectric materials exhibit the two distinct electromechanical effects: direct piezoelectric effect and converse piezoelectric effect. The former is fundamental for many sensor applications, e.g., accelerometers, force/pressure transducers, etc; the latter creates a basis for precision actuation and control applications. Due to their versatility in both sensor and actuator applications, piezoelectric materials are also widely used in modern smart structures and structronic systems. As the functional requirements become higher, the geometry of the piezoelectric devices also extends from the one-dimensional (1D) rods, 1D rings, to two-dimensional (2D) flat plates, and 2D curved continua, e.g., cylindrical shells, conical shells, spherical shells, etc (Tzou, 1993). The linear piezoelastic phenomena and theories have been studied for years (Chau, 1986; Dökmeci, 1983; Drumheller and Kalnins, 1970; Mindlin, 1972; Rogacheva, 1994; Senik and Kudriavtsev, 1980; Tzou and Gadre, 1989). An umbrella linear piezo-thermo-elastic shell theory based on a double-curvature generic shell was proposed and the derived governing equations can be easily simplified to account for many standard piezoelectric continua (Tzou and Howard, 1994). The linear thermo-electromechanical behavior and precision position control of distributed piezoelectric sensors and actuators were also investigated (Koppe et al., 1998; Tzou and Ye, 1994). As the deformation goes beyond the linear elastic range, growing deformation geometric nonlinearity also should be considered. Geometrical nonlinearity of elastic shells was investigated over the years (Librescu, 1987; Palazotto and Dennis, 1992; Pietraszkiewicz, 1979; Chia, 1980). Pai et al. (1993) proposed a nonlinear model for a piezoelectric plate. However, geometrical nonlinearity of anisotropic piezothermoelastic shells simultaneously exposed to mechanical, electric, and thermal fields have not been fully investigated (Tzou and Bao, 1997; Tzou and Zhou, 1995). This paper presents an advanced nonlinear piezo(electric)-thermoelastic shell theory and a detailed analysis of electromechanical coupling of distributed piezoelectric sensors and actuators laminated on shell structures of various curvatures.

2. Piezo-thermoelastic constitutive equations and nonlinear piezo-thermoelastic flexible shell continua

A mathematical model of nonlinear piezo(electric)-thermoelastic shell continuum revealing large-deformation geometric nonlinearity offers an umbrella approach that can be easily extended to cover nonlinear shells, (e.g., spherical, conical, cylindrical, etc.) and plates (e.g., rectangular, circular, etc), linear shells and plates, and many other shapes (e.g., arches, rings, beams, etc.). Figure 1 shows the three fundamental double-curvature flexible shell continua: a) piezo(electric)-thermoelastic shell, b) elastic shell with distributed sensor and actuator layers, and c) composite piezothermoelastic shell, and their derivative shapes based on simplification procedures (Tzou, 1993). Thus, fundamental theories, distributed control mechanisms, and solution procedures, etc. constructed for the generic nonlinear flexible shell continuum can be easily applied to a large number of flexible shell and non-shell structures. In this section, fundamental piezo(electric)-thermoelectromechanical properties of a piezoelectric continuum are briefly reviewed. A generic theory based on a nonlinear piezo(electric)-thermoelastic shell with the von Karman geometric nonlinearity is proposed and its governing equations are derived. Figure 1a shows a generic double-curvature flexible shell subjected to mechanical, electric, and temperature excitations; the shell is defined in a tri-orthogonal curvilinear coordinate system in which α_1 and α_2 define the in-plane axes and α_3 defines the transverse direction.

2.1. Piezo(electric)-thermoelastic constitutive equations

The piezo-thermoelectromechanical constitutive relations of a generic piezo-thermoelastic shell continuum are governed by the three fundamental equations (Tzou and Howard, 1994)

— stress equation

$$\boldsymbol{T} = \mathbf{c}\boldsymbol{S} - \mathbf{e}^{\top}\boldsymbol{E} - \boldsymbol{\lambda}\theta \tag{2.1}$$

— electric displacement equation

$$\boldsymbol{D} = \mathbf{e}\boldsymbol{S} - \boldsymbol{\varepsilon}\boldsymbol{E} - \boldsymbol{p}\theta \tag{2.2}$$

— thermal entropy equation

$$\mathcal{I} = \boldsymbol{\lambda}^{\top}\boldsymbol{S} - \boldsymbol{p}^{\top}\boldsymbol{E} - \alpha_v\theta \tag{2.3}$$

where

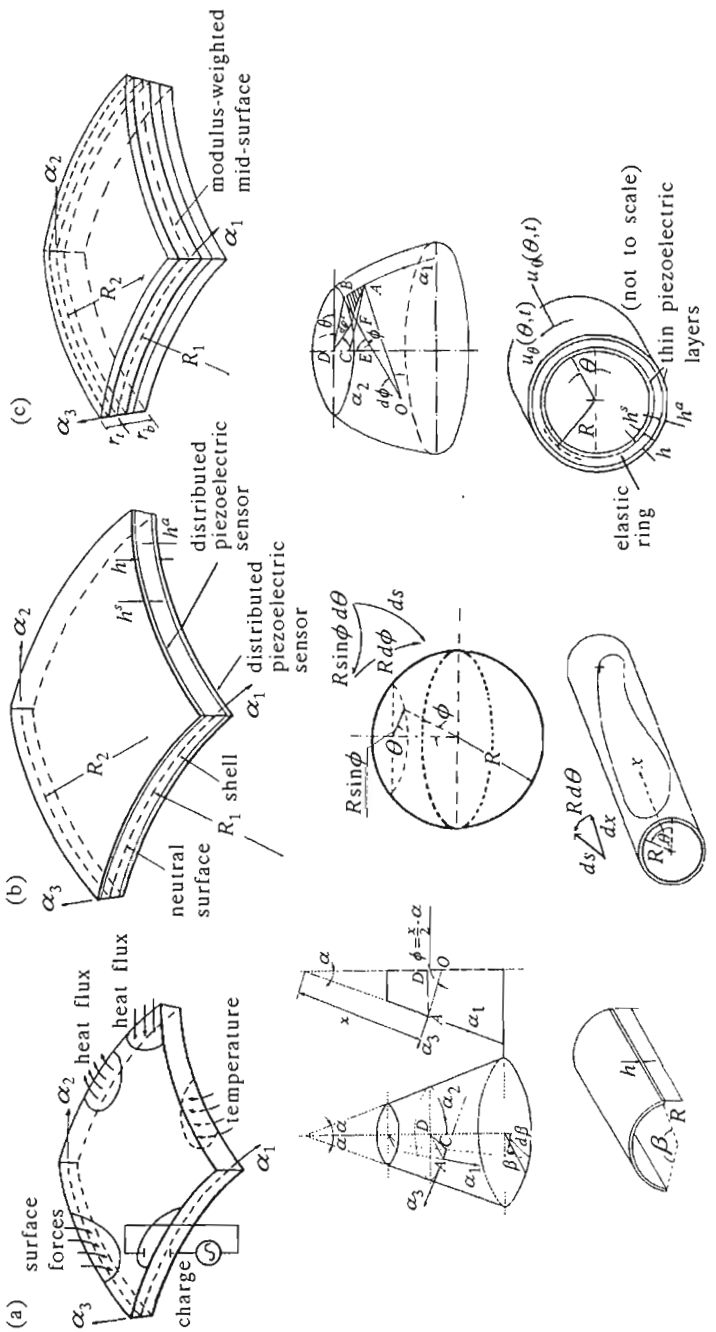

Fig. 1. Three generic double-curvature shells and their derived shell continua

$\boldsymbol{T}$ – stress vector
$\boldsymbol{S}$ – strain vector
$\boldsymbol{E}$ – electric field vector
$\boldsymbol{D}$ – electric displacement vector
$\mathbf{c}$ – elastic stiffness coefficient matrix
$\mathbf{e}$ – piezoelectric coefficient matrix
$\boldsymbol{\varepsilon}$ – dielectric permittivity matrix
$\mathcal{I}$ – thermal entropy density
θ – temperature rise ($\theta = \Theta - \Theta_0$ where Θ is the absolute temperature and Θ_0 the temperature of the natural state in which stresses and strains are zero)
$\boldsymbol{\lambda}$ – stress-temperature coefficient vector
$\boldsymbol{p}$ – pyroelectric coefficient vector
α_v – material constant ($\alpha_v = \rho c_v/\Theta_0$ where ρ is the material density and c_v is the specific heat at a constant volume).

The electric fields E_1, E_2, E_3 and the electric potential ϕ in the shell curvilinear shell coordinate system are defined by

$$\{E_i\} = -[f_{ii}]\left\{\frac{\partial \phi}{\partial \alpha_i}\right\} \qquad i = 1,2,3$$

where

$$f_{ii}(\alpha_1, \alpha_2, \alpha_3) = \begin{cases} A_i\left(1 + \dfrac{\alpha_3}{R_i}\right) & \text{for } i = 1,2 \\ 1 & \text{for } i = 3 \end{cases}$$

is a finite distance measured from the reference surface; A_1 and A_2 are the Lamé parameters; R_1 and R_2 are the radii of curvature of the α_1 and α_2 axes on the neutral surface defined by $\alpha_3 = 0$. The Lamé parameters (A_1 and A_2) and two radii (R_1 and R_2) are the four essential parameters used in simplification and application of the generic shell theory to other geometries and shell/non-shell continua (Tzou, 1993). Nonlinear piezo-thermoelastic shells are evaluated and generic thermo-electromechanical equations are defined in the next section.

2.2. Large deformation geometric nonlinearity

The shape transformation and imposed shape control often involves large deformations; i.e., geometric nonlinearity. A generic nonlinear deflection U_i in the ith direction of the shell can be expressed as a sum of (in-plane) membrane displacement $u_i(\alpha_1, \alpha_2, t)$ and higher order nonlinear shear deformation effect

represented by the sum of angular displacements $\beta_{ij}(\alpha_1, \alpha_2, t)$

$$U_i(\alpha_1, \alpha_2, \alpha_3, t) = u_i(\alpha_1, \alpha_2, t) + \sum_{j=1}^{m} \alpha_3^j \beta_{ij}(\alpha_1, \alpha_2, t) \tag{2.4}$$

where β_{11} and β_{21} represent the angles of rotation in the positive sense of α_1 and α_2 axes, respectively; and $\beta_{3j} = 0$. This formula includes higher order nonlinear shear deformation effects. However, according to the Love-Kirchhoff thin shell assumptions and a linear displacement approximation (first order shear deformation theory), only the first term is kept in the equation, i.e., $m = 1$. The displacements and angles of rotation are independent variables in thick shells. However, the angles of rotation are dependent variables in thin shells, and they can be derived on the thin shell assumptions that the transverse normal strain S_3 is negligible and the shear strains S_4 and S_5 are equal zero. Based on the thin shell assumptions, the angles of rotation $\beta_1 = \beta_{11}$ and $\beta_2 = \beta_{21}$ are derived from the transverse shear strain equations, i.e., $S_4 = 0$ and $S_5 = 0$. Thus, the angles of rotation are defined as

$$\beta_i = \frac{u_i}{R_i} - \frac{1}{A_i}\frac{\partial u_3}{\partial \alpha_i} \qquad i = 1, 2$$

In general, since $\alpha_3/R_1 \ll 1$ and $\alpha_3/R_2 \ll 1$, the ratios of the finite distance to the radius of curvature are negligible, i.e., $f_{11} \approx A_1$ and $f_{22} \approx A_2$.

Although it is assumed that the piezoelectric shell experiences large deformations in the three axial directions, however, in reality, the in-plane deflections are much smaller than the transverse deflection. Thus, the nonlinear effects due to the in-plane large deflections are usually neglected, i.e., the von Karman-type assumptions (Palazotto and Dennis, 1992; Chia, 1980) are accepted. The nonlinear strain-displacement relations for a thin shell revealing a large transverse deflection u_3 include both the linear effect (denoted by the superscript l), and the nonlinear one (denoted by the superscript n), induced by the large deformation

$$\{S_i\} = \left(\{s_i^0\}^l + \{s_i^0\}^n\right) + \alpha_3\{k_i\} \qquad i = 1, 2, 6 \tag{2.5}$$

where the subscripts 1 and 2, respectively, denote two normal strains and 6 represents the in-plane shear strain. Detailed membrane and bending strains (s_i^0 and k_i) are expressed as functions of the displacements u_i, the Lamé parameters (A_1 and A_2), and the two radii (R_1 and R_2)

$$
\begin{aligned}
s_1^0 &= \frac{1}{A_1}\frac{\partial u_1}{\partial \alpha_1} + \frac{u_2}{A_1 A_2}\frac{\partial A_1}{\partial \alpha_2} + \frac{u_3}{R_1} + \frac{1}{2A_1^2}\left(\frac{\partial u_3}{\partial \alpha_1}\right)^2 \\
s_2^0 &= \frac{1}{A_2}\frac{\partial u_2}{\partial \alpha_2} + \frac{u_1}{A_1 A_2}\frac{\partial A_2}{\partial \alpha_1} + \frac{u_3}{R_2} + \frac{1}{2A_2^2}\left(\frac{\partial u_3}{\partial \alpha_2}\right)^2 \\
s_6^0 &= \frac{1}{A_2}\frac{\partial u_1}{\partial \alpha_2} + \frac{1}{A_1}\frac{\partial u_2}{\partial \alpha_1} - \frac{u_1}{A_1 A_2}\frac{\partial A_1}{\partial \alpha_2} - \frac{u_2}{A_1 A_2}\frac{\partial A_2}{\partial \alpha_1} + \frac{1}{A_1 A_2}\frac{\partial u_3}{\partial \alpha_1}\frac{\partial u_3}{\partial \alpha_2} \\
k_1 &= \frac{1}{A_1}\frac{\partial}{\partial \alpha_1}\left(\frac{u_1}{R_1} - \frac{1}{A_1}\frac{\partial u_3}{\partial \alpha_1}\right) + \frac{1}{A_1 A_2}\left(\frac{u_2}{R_2} - \frac{1}{A_2}\frac{\partial u_3}{\partial \alpha_2}\right)\frac{\partial A_1}{\partial \alpha_2} \\
k_2 &= \frac{1}{A_2}\frac{\partial}{\partial \alpha_2}\left(\frac{u_2}{R_2} - \frac{1}{A_2}\frac{\partial u_3}{\partial \alpha_2}\right) + \frac{1}{A_1 A_2}\left(\frac{u_1}{R_1} - \frac{1}{A_1}\frac{\partial u_3}{\partial \alpha_1}\right)\frac{\partial A_2}{\partial \alpha_1} \\
k_6 &= \frac{1}{A_2}\frac{\partial}{\partial \alpha_2}\left(\frac{u_1}{R_1} - \frac{1}{A_1}\frac{\partial u_3}{\partial \alpha_1}\right) + \frac{1}{A_1}\frac{\partial}{\partial \alpha_1}\left(\frac{u_2}{R_2} - \frac{1}{A_2}\frac{\partial u_3}{\partial \alpha_2}\right) + \\
&- \frac{1}{A_1 A_2}\left(\frac{u_1}{R_1} - \frac{1}{A_1}\frac{\partial u_3}{\partial \alpha_1}\right)\frac{\partial A_1}{\partial \alpha_2} - \frac{1}{A_1 A_2}\left(\frac{u_2}{R_2} - \frac{1}{A_2}\frac{\partial u_3}{\partial \alpha_2}\right)\frac{\partial A_2}{\partial \alpha_1}
\end{aligned}
\tag{2.6}
$$

Note that the quadratic terms (nonlinear terms) inside the brackets are contributed by the large deflection. The membrane force resultants N_{ij} and the bending moments M_{ij} of the piezothermoelastic shell, Fig.1a, are defined by the elastic, electric, and the temperature components

$$
\begin{bmatrix} N_{11} \\ N_{22} \\ N_{12} \\ M_{11} \\ M_{22} \\ M_{12} \end{bmatrix} = \begin{bmatrix} A_{11} & A_{12} & A_{16} & 0 & 0 & 0 \\ A_{12} & A_{22} & A_{26} & 0 & 0 & 0 \\ A_{16} & A_{26} & A_{66} & 0 & 0 & 0 \\ 0 & 0 & 0 & D_{11} & D_{12} & D_{16} \\ 0 & 0 & 0 & D_{12} & D_{22} & D_{26} \\ 0 & 0 & 0 & D_{16} & D_{26} & D_{66} \end{bmatrix} \begin{bmatrix} s_1^0 \\ s_2^0 \\ s_6^0 \\ k_1 \\ k_2 \\ k_6 \end{bmatrix} - \begin{bmatrix} N_{11}^e \\ N_{22}^e \\ N_{12}^e \\ M_{11}^e \\ M_{22}^e \\ M_{12}^e \end{bmatrix} - \begin{bmatrix} N_{11}^\theta \\ N_{22}^\theta \\ N_{12}^\theta \\ M_{11}^\theta \\ M_{22}^\theta \\ M_{12}^\theta \end{bmatrix} \tag{2.7}
$$

Furthemore, the membrane force resultants N_{ij} and the bending moments M_{ij} of the piezothermoelastic laminated compsite shell, see Fig.1c, can be defined as follows (Tzou and Bao, 1997)

$$
\begin{bmatrix} N_{11} \\ N_{22} \\ N_{12} \\ M_{11} \\ M_{22} \\ M_{12} \end{bmatrix} = \begin{bmatrix} A_{11} & A_{12} & A_{16} & B_{11} & B_{12} & B_{16} \\ A_{12} & A_{22} & A_{26} & B_{12} & B_{22} & B_{26} \\ A_{16} & A_{26} & A_{66} & B_{16} & B_{26} & B_{66} \\ B_{11} & B_{12} & B_{16} & D_{11} & D_{12} & D_{16} \\ B_{12} & B_{22} & B_{26} & D_{12} & D_{22} & D_{26} \\ B_{16} & B_{26} & B_{66} & D_{16} & D_{26} & D_{66} \end{bmatrix} \begin{bmatrix} s_1^0 \\ s_2^0 \\ s_6^0 \\ k_1 \\ k_2 \\ k_6 \end{bmatrix} - \begin{bmatrix} N_{11}^e \\ N_{22}^e \\ N_{12}^e \\ M_{11}^e \\ M_{22}^e \\ M_{12}^e \end{bmatrix} - \begin{bmatrix} N_{11}^\theta \\ N_{22}^\theta \\ N_{12}^\theta \\ M_{11}^\theta \\ M_{22}^\theta \\ M_{12}^\theta \end{bmatrix} \tag{2.8}
$$

where A_{ij}, B_{ij} and D_{ij} are the extensional coupling, and bending stiffness constants. The superscripts e and θ, respectively, denote the electric and temperature components. The membrane strains and the bending strains are coupled by the coupling stiffness coefficients B_{ij} in the elastic force/moment resultants. N_{ij}^e and N_{ij}^θ are the electric and temperature induced forces; M_{ij}^e and M_{ij}^θ are the electric and temperature induced moments, respectively. In actuator applications, these electric forces and moments are used to control static and dynamic characteristics of the shell. These strain/displacement relations, membrane force resultants, bending moment resultants, etc. are used in Hamilton's equation to derive the thermo-electromechanical equations and boundary conditions of nonlinear piezothermoelastic shells. Although it is assumed that the transverse shear deflections can be neglected, the integrated effect of the transverse shear stress resultants Q_{13} and Q_{23} are not neglected. Note, that the effects of rotational inertia can be neglected in thin shells without large rotational effects. Thus, the original set of governing equations can be reduced to three governing equations.

2.3. Hamilton's principle and nonlinear system equations

Hamilton's principle is used to derive the thermo-electromechanical shell equations and boundary conditions of the piezothermoelastic shell continuum. Hamilton's principle assumes that the energy variations over an arbitrary period of time are zero. Considering all energies, one can write Hamilton's equation as

$$\delta \int_{t_0}^{t_1} \left[\int_V \left(\frac{1}{2}\rho \dot{\boldsymbol{U}}_j \dot{\boldsymbol{U}}_j - H(S_i, E_i, \Theta) + \mathcal{I}\Theta \right) dV - \int_S (\boldsymbol{t}_j \boldsymbol{U}_j - Q_j \phi)\, dS \right] dt = 0 \quad (2.9)$$

where

ρ	–	mass density
H	–	electric enthalpy
$\boldsymbol{t}_j$	–	surface traction in the α_j direction
Q_j	–	surface electric charge
ϕ	–	electrical potential
V, S	–	volume and surface of the piezothermoelastic shell continuum, respectively
$\boldsymbol{U}_j, \dot{\boldsymbol{U}}_j$	–	displacement and velocity vectors.

It is assumed that only the transverse electric field E_3 is considered in the analysis. Substituting all energy expressions into Hamilton's equation and carrying out all variations, one can derive the nonlinear piezothermoelastic shell

equations and boundary conditions of the piezothermoelastic shell continuum

$$
\begin{aligned}
&-\frac{\partial(N_{11}A_2)}{\partial\alpha_1}+N_{22}\frac{\partial A_2}{\partial\alpha_1}-\frac{\partial(N_{21}A_1)}{\partial\alpha_2}-N_{12}\frac{\partial A_1}{\partial\alpha_2}-\frac{1}{R_1}\Big[\frac{\partial(M_{11}A_2)}{\partial\alpha_1}+\\
&-M_{22}\frac{\partial A_2}{\partial\alpha_1}+\frac{\partial(M_{21}A_1)}{\partial\alpha_2}+M_{12}\frac{\partial A_1}{\partial\alpha_2}\Big]+A_1A_2\rho h\ddot{u}_1=A_1A_2F_1\\
&-\frac{\partial(N_{22}A_1)}{\partial\alpha_2}+N_{11}\frac{\partial A_1}{\partial\alpha_2}-\frac{\partial(N_{12}A_2)}{\partial\alpha_1}-N_{21}\frac{\partial A_2}{\partial\alpha_1}-\frac{1}{R_2}\Big[\frac{\partial(M_{22}A_1)}{\partial\alpha_2}+\\
&-M_{11}\frac{\partial A_1}{\partial\alpha_2}+\frac{\partial(M_{12}A_2)}{\partial\alpha_1}+M_{21}\frac{\partial A_2}{\partial\alpha_1}\Big]+A_1A_2\rho h\ddot{u}_2=A_1A_2F_2\\
&-\frac{\partial}{\partial\alpha_1}\Big[\frac{1}{A_1}\Big(\frac{\partial(M_{11}A_2)}{\partial\alpha_1}-M_{22}\frac{\partial A_2}{\partial\alpha_1}+\frac{\partial(M_{21}A_1)}{\partial\alpha_2}+M_{12}\frac{\partial A_1}{\partial\alpha_2}\Big)\Big]+\\
&-\frac{\partial}{\partial\alpha_2}\Big[\frac{1}{A_2}\Big(\frac{\partial(M_{22}A_1)}{\partial\alpha_2}-M_{11}\frac{\partial A_1}{\partial\alpha_2}+\frac{\partial(M_{12}A_2)}{\partial\alpha_1}+M_{21}\frac{\partial A_2}{\partial\alpha_1}\Big)\Big]+\\
&+A_1A_2\Big(\frac{N_{11}}{R_1}+\frac{N_{22}}{R_2}\Big)+A_1A_2\rho h\ddot{u}_3-\Big[\Big(\frac{\partial(N_{11}A_2/A_1)}{\partial\alpha_1}+\frac{\partial N_{12}}{\partial\alpha_2}\Big)\frac{\partial u_3}{\partial\alpha_1}+\\
&+\Big(\frac{\partial(N_{22}A_1/A_2)}{\partial\alpha_2}+\frac{\partial N_{12}}{\partial\alpha_1}\Big)\frac{\partial u_3}{\partial\alpha_2}+2N_{12}\frac{\partial^2u_3}{\partial\alpha_1\partial\alpha_2}+N_{11}\frac{A_2}{A_1}\frac{\partial^2u_3}{\partial\alpha_1^2}+\\
&+N_{22}\frac{A_1}{A_2}\frac{\partial^2u_3}{\partial\alpha_2^2}\Big]=A_1A_2F_3
\end{aligned}
\tag{2.10}
$$

Note that all terms inside the brachets are contributed by the nonlinear effects and the *nonlinear influence* on the transverse equation u_3 is significant. The thermo-electromechanical shell equations look similar to those for the standard shell. However, the force and moment expressions defined by mechanical, thermal, and electric effects are much more complicated than the conventional elastic expressions, Eqs (2.7) and (2.8). Substituting the formulae for N_{11}, N_{22}, N_{12}, M_{11}, M_{22}, M_{12} into the above equations yields the thermo-electromechanical equations defined in the reference displacements u_1, u_2, u_3. Recall, that the transverse shear deformation and the rotational inertia effects are not considered. The electric terms, forces and moments, can be used in controlling the mechanical and/or temperature induced excitations (Tzou and Ye, 1994). Note, that all elastic, electric, and thermal related terms can also appear in boundary conditions. These electric terms can be used, combined with control algorithms, as control forces/moments counteracting mechanical and temperature induced vibrations in distributed structural control of shells (Tzou et al., 1999). Applications and simplifications of the nonlinear piezo-

thermoelastic shell equations can be demonstrated in the two ways:

- material simplifications and
- geometrical simplifications (Tzou, 1993; Tzou and Bao, 1996).

In the next section, detailed distributed sensing and control mechanisms of distributed shell sensor/actuator layers are investigated.

3. Distributed sensing of nonlinear shells

Distributed piezoelectric layers laminated on the generic nonlinear shell respond to shell strain variations and as a result generate electric signals based on the direct piezoelectric effect, see Fig.1b. The open-circuit signal ϕ^s is a function of induced local strains S_{ij} and the piezoelectric constants d_{ij}

$$\phi^s = \frac{h^s}{S^e}\int_{\alpha_1}\int_{\alpha_2}(d_{31}S_{11}^s + d_{32}S_{22}^s + d_{36}S_{12}^s)A_1A_2\,d\alpha_1 d\alpha_2 \tag{3.1}$$

where

h^s – sensor thickness
S^e – effective electrode area
A_1, A_2 – Lamé costants.

The surface integration represents the total charge generated over the effective electrode area defined by the α_1 and α_2 axes. Note, that since the sensor is spatially distributed, the signal is averaged over the total effective electrode area (Tzou et al., 1993). The strain can be divided into the membrane strain and the bending strain. Thus, the sensor signal resulting from a nonlinear shell can be further expressed as

$$\begin{aligned}
\phi^s = \frac{h^s}{S^e}\int_{\alpha_1}\int_{\alpha_2}\Big\{ & d_{31}\Big\{\frac{1}{A_1}\frac{\partial u_1}{\partial\alpha_1} + \frac{u_2}{A_1A_2}\frac{\partial A_1}{\partial\alpha_2} + \frac{u_3}{R_1} + \frac{1}{2A_1^2}\Big(\frac{\partial u_3}{\partial\alpha_1}\Big)^2 + \\
& + r^s\Big[\frac{1}{A_1}\frac{\partial}{\partial\alpha_1}\Big(\frac{u_1}{R_1} - \frac{1}{A_1}\frac{\partial u_3}{\partial\alpha_1}\Big) + \frac{1}{A_1A_2}\Big(\frac{u_2}{R_2} - \frac{1}{A_2}\frac{\partial u_3}{\partial\alpha_2}\Big)\frac{\partial A_1}{\partial\alpha_2}\Big]\Big\} + \\
& + d_{32}\Big\{\frac{1}{A_2}\frac{\partial u_2}{\partial\alpha_2} + \frac{u_1}{A_1A_2}\frac{\partial A_2}{\partial\alpha_1} + \frac{u_3}{R_2} + \frac{1}{2A_2^2}\Big(\frac{\partial u_3}{\partial\alpha_2}\Big)^2 + \\
& + r^s\Big[\frac{1}{A_2}\frac{\partial}{\partial\alpha_2}\Big(\frac{u_2}{R_2} - \frac{1}{A_2}\frac{\partial u_3}{\partial\alpha_2}\Big) + \frac{1}{A_1A_2}\Big(\frac{u_1}{R_1} - \frac{1}{A_1}\frac{\partial u_3}{\partial\alpha_1}\Big)\frac{\partial A_2}{\partial\alpha_1}\Big]\Big\} +
\end{aligned} \tag{3.2}$$

$$+d_{36}\Big\{\frac{1}{A_2}\frac{\partial u_1}{\partial \alpha_2}+\frac{1}{A_1}\frac{\partial u_2}{\partial \alpha_1}-\frac{u_1}{A_1A_2}\frac{\partial A_1}{\partial \alpha_2}-\frac{u_2}{A_1A_2}\frac{\partial A_2}{\partial \alpha_1}+\frac{1}{A_1A_2}\frac{\partial u_3}{\partial \alpha_1}\frac{\partial u_3}{\partial \alpha_2}+$$

$$+r^s\Big[\frac{A_1}{A_2}\frac{\partial}{\partial \alpha_2}\Big(\frac{u_1}{R_1A_1}-\frac{1}{A_1^2}\frac{\partial u_3}{\partial \alpha_1}\Big)+\frac{A_2}{A_1}\frac{\partial}{\partial \alpha_1}\Big(\frac{u_2}{R_2A_2}-\frac{1}{A_2^2}\frac{\partial u_3}{\partial \alpha_2}\Big)+$$

$$-\frac{1}{A_1A_2}\Big(\frac{u_1}{R_1}-\frac{1}{A_1}\frac{\partial u_3}{\partial \alpha_1}\Big)\frac{\partial A_1}{\partial \alpha_2}-\frac{1}{A_1A_2}\Big(\frac{u_2}{R_2}-\frac{1}{A_2}\frac{\partial u_3}{\partial \alpha_2}\Big)\frac{\partial A_2}{\partial \alpha_1}\Big]\Big\}\Big\}\cdot$$

$$\cdot A_1A_2\,d\alpha_1 d\alpha_2$$

where

u_i – displacements

R_i – radius of curvature of the ith axis

r^s – sensor location away from the shell neutral surface.

The terms following r^s represent the bending strain component; while the others denote the membrane strain component. The membrane strain component is related to in-plane oscillations and the bending component is related to bending oscillation of the generic shell. Note that the large deformation effect is included with the membrane strains, the quadratic terms, based on the von Karman geometric nonlinearity theory. To demonstrate the distributed sensing concept, distributed sensing behavior of shells is investigated later.

4. Distributed control of nonlinear shells

Distributed control of nonlinear shell continua requires different approaches as compared with that to the discrete parameter systems. Distributed control effectiveness of shells suggests that the overall control effect can be divided into the two major control actions:

- membrane control action and
- bending control action.

Usually, the membrane control action dominates the lower-mode control of deep shells, e.g., cylindrical shell, and the bending control action dominates the control of higher deep-shell modes and all modes of zero-curvature continua, e.g., plates and beams (Tzou et al., 1998). (These phenomena will be demonstrated in the Case Studies presented later.) Assume that the control components N_{ij}^e in the flexible shell equation can be represented by a control function $N_{ij}^e = L_i^a(\phi_1, \phi_2, \phi_3) = L_i^a(\phi_i)$, $i = 1, 2, 3$, where ϕ_i is the control potential. Define a distributed feedback function $L_i^a(\phi_i) = \{\Lambda_i(\alpha_1, \alpha_2, t)\}$,

$i = 1, 2, 3$, where Λ_i can be displacement, velocity, acceleration or combination of several reference factors. Expanding the distributed feedback function in the modal domain

$$L_i^a(\phi_i) = \sum_{k=1}^{\infty} G_{ik}^*(\alpha_1, \alpha_2)\eta_k^*(t) \qquad i = 1, 2, 3$$

one can express the distributed control force as

$$\widehat{F}_k = \frac{1}{\rho h N_k} \int_{\alpha_1} \int_{\alpha_2} \sum_{j=1}^{3} \sum_{k=1}^{\infty} G_{ik}^*(\alpha_1, \alpha_2)\eta_k^*(t) U_{jk}(\alpha_1, \alpha_2) A_1 A_2 \, d\alpha_1 d\alpha_2 \tag{4.1}$$

where

$$N_k = \int_{\alpha_1} \int_{\alpha_2} \sum_{j=1}^{3} U_{jk}^2(\alpha_1, \alpha_2) A_1 A_2 \, d\alpha_1 d\alpha_2$$

and

U_{jk} – mode shape function
$G_{ik}^*(\alpha_1, \alpha_2)$ – spatial gain function
η_k^* – modal coordinate of the kth mode.

Assuming that the distributed control force is velocity dependent and the gain factor G_{ik}^* is a constant, one can derive the modal domain control equations as

$$\ddot{\eta}_k + \frac{1}{\rho h}\Big(c - \frac{G_k^v}{N_k} \int_{\alpha_1} \int_{\alpha_2} U_{jk}^2 A_1 A_2 \, d\alpha_1 d\alpha_2\Big)\dot{\eta}_k + \omega_k^2 \eta_k = 0 \tag{4.2}$$

Accordingly, modal responses of nonlinear flexible shell continua can be independently controlled. The spatial shapes of required actuators can also be represented by the spatial gain function such that a single mode or combination of natural modes can be optimally controlled by means of limited distributed actuators (Tzou et al., 1993, 1994). The case studies exploiting detailed sensing and control mechanisms are presented below.

5. Sensing and control mechanisms of shells with various curvatures

Adaptive structures and shape control often involve shape transformation from one geometry to the other, in order to achieve specific functional advantages in practical applications, such as flow control, lift control, vibration

control, etc. Plates are zero-curvature *shells*, per se; cylinders can be formed with a plate wrapped around 360° and sealed at the connection. Accordingly, transforming a shallow cylindrical shell to a full-closed cylinder would be a good example of revealing detailed sensing and control mechanisms in the shape transformation of adaptive shells. Fig.2 shows a shape transformation of a shallow cylindrical shell to a cylinder. However, since the purpose is to evaluate the curvature effect to distributed sensing and control characteristics, the external nonlinear force and large deformation effects are not considered in the analysis, although the nonlinear theory was presented earlier.

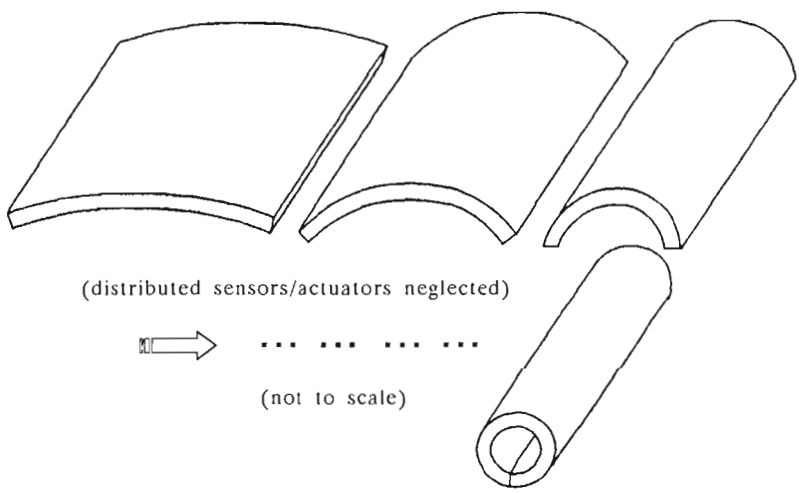

Fig. 2. Shape transformation of a cylindrical shell

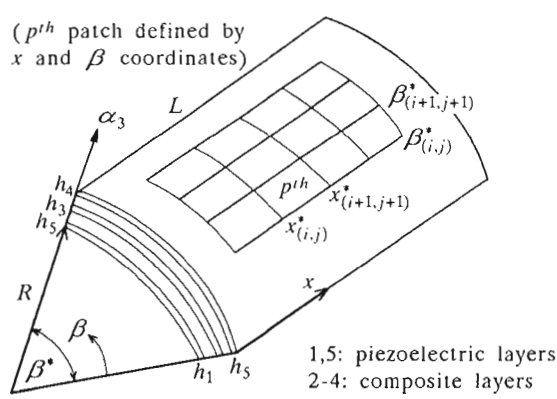

Fig. 3. Composite flexible cylindrical shell with distributed piezoelectric layers

The coordinate system of a cylindrical shell is defined in Fig.3, in which x denotes the length direction, β the circumferential direction, and α_3 the transverse direction. The Lamé constants are $A_1 = 1$ and $A_2 = R$; the radii of curvature are $R_1 = \infty$ and $R_2 = R$. Distributed piezoelectric layers laminated on elastic continua can be used as distributed sensors and/or actuators, see Fig.3.

Substituting the Lamé constants and radii of curvature into the nonlinear flexible shell piezo-thermoelectromecahnical equations yields the three governing equations of flexible cylindrical shells

$$
\begin{aligned}
&-\frac{\partial N_{xx}}{\partial x} - \frac{1}{R}\frac{\partial N_{x\beta}}{\partial \beta} + \rho h \ddot{u}_1 = F_1 + \frac{\partial N^c_{xx}}{\partial x} \\
&-\frac{\partial N_{x\beta}}{\partial x} - \frac{1}{R}\frac{\partial N_{\beta\beta}}{\partial \beta} - \frac{1}{R}\Big(\frac{\partial M_{x\beta}}{\partial x} + \frac{1}{R}\frac{\partial M_{\beta\beta}}{\partial \beta}\Big) + \rho h \ddot{u}_2 = \\
&= F_2 + \frac{1}{R}\frac{\partial N^c_{\beta\beta}}{\partial \beta} + \frac{1}{R^2}\frac{\partial M^c_{\beta\beta}}{\partial \beta} \qquad (5.1) \\
&-\frac{\partial^2 M_{xx}}{\partial x^2} - \frac{2}{R}\frac{\partial^2 M_{x\beta}}{\partial x^2} - \frac{1}{R^2}\frac{\partial^2 M_{\beta\beta}}{\partial \beta^2} + \frac{N_{\beta\beta}}{R} + \rho h \ddot{u}_3 = \\
&= F_3 + \frac{\partial^2 M^c_{xx}}{\partial x^2} + \frac{1}{R^2}\frac{\partial^2 M^c_{\beta\beta}}{\partial \beta^2} - \frac{N^c_{\beta\beta}}{R}
\end{aligned}
$$

The forces and moments are defined by

$$
\begin{aligned}
N_{ij} &= N^m_{ij} + N^e_{ij} + N^\theta_{ij} \\
M_{ij} &= M^m_{ij} + M^e_{ij} + M^\theta_{ij}
\end{aligned}
$$

in Eq (2.7) for single layer piezo-thermoelastic shells and in Eq (2.8) for multi-layer composite shells, see Fig.3. Injecting high voltages into the distributed piezoelectric actuators induces two major control actions. One is the in-plane membrane control force(s) and the other is the out-of-plane bending control moment(s). In general, the control moments are essential in zero-curvature planar structures, e.g., plates and beams; the membrane control forces are effective in shells. In this study, detailed sensing and control characteristics of the cylindrical shell are evaluated with respect to the curvature changes, from shallow shells to deep shells ($30° \rightarrow 120°$).

Since sensing and control effectiveness is natural mode dependent, natural frequencies of the cylindrical shells (i.e., $30°$, $60°$, $90°$, $120°$, and $150°$) are

presented in Fig.4. It shows that the natural frequency continuously increases as the mode varies from lower to higher modes of shallow shells (e.g., 30°, 60°), which indicates that the bending behavior dominates the dynamics. However, as the curvature increases to deep shells (e.g., 90°, 120°, and 150°), the natural frequency drops for the first few natural modes and takes off at higher modes. This behavior especially is significant for the deep shell (150°), due to the membrane behavior dominating the first few natural modes. As the mode increases, the bending behavior becomes prominent at higher natural modes.

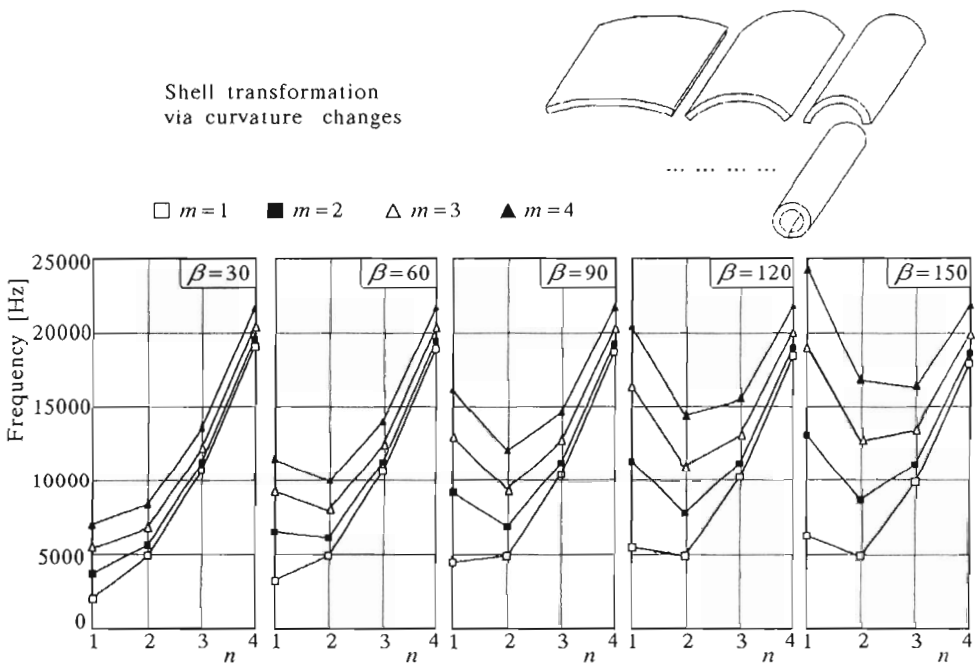

Fig. 4. Frequency variation of the cylindrical shells

5.1. Distributed sensor characteristics

It is assumed that a piezoelectric layer is laminated on the shells and the sensing characteristics of these shells are investigated in this section. Recall that the total sensing signal is contributed by the two components: the membrane component and the bending component. Thus, the signal generations from the membrane and the bending components of the shells (i.e., 30°, 60°, 90°, 120°, and 150°) are respectively calculated and plotted in Fig.5. Note that the bottom plots denote the signals generated from the bending effect,

the middle plots show the signals generated from the membrane effect, and the top plots show the total signals. It can be seen from the figures, that the membrane signal increases as the curvature increases; the bending signal remains unchanged in all shell variations since the distance from the neutral surface to the sensor layer is constant in all cases. As discussed previously, the bending strain component is prominent in shallow shells and the membrane strain component is prominent in deep shells. This phenomenon also reflects in the signal generation. The membrane signal increases as the curvature increases and this signal becomes the dominating one in deep shells.

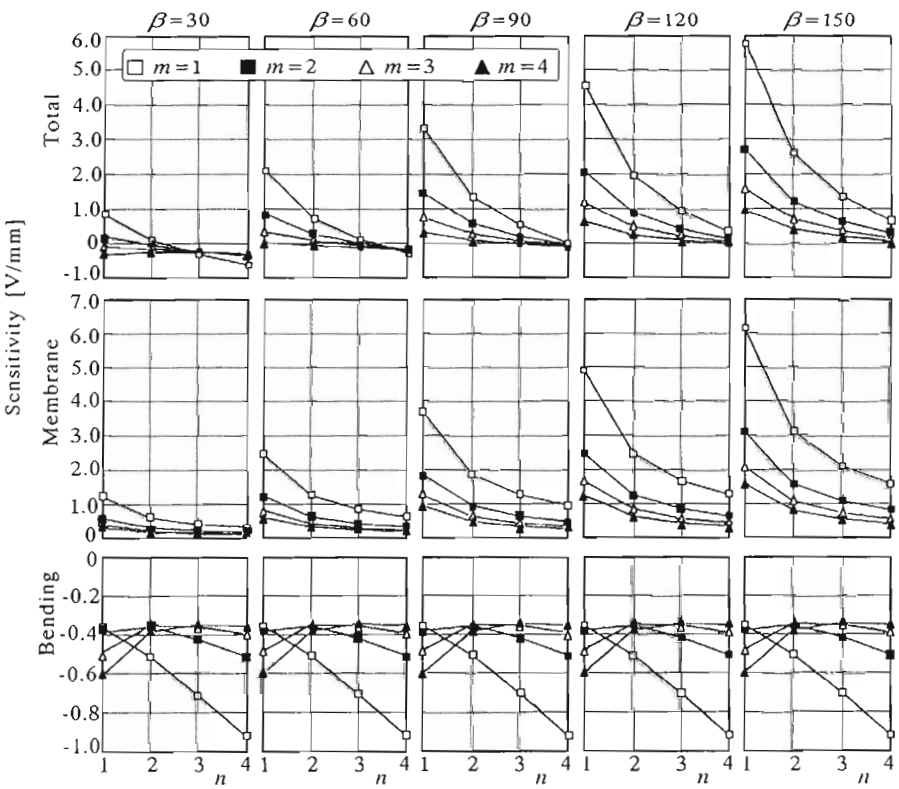

Fig. 5. Distributed sensing characteristics

5.2. Distributed actuator characteristics

Furthermore, distributed control characteristics of piezoelectric laminated shells are investigated. Similar to the distributed sensing characteristics, there are two essential contributing components (i.e., the membrane component and

the bending component) influencing the overall control electromechanics of the shells. These two components are also calculated and plotted in Fig.6. Again, the bottom plots represents the bending actuation factors, the middles show the membrane actuation factors, and the tops denote the total effect. Analytical results suggest that the membrane control effect increases as the curvature increases, indicating that the membrane control effect dominates the control of lower natural modes in deep shells and the bending control effect dominates the control of shallow shells.

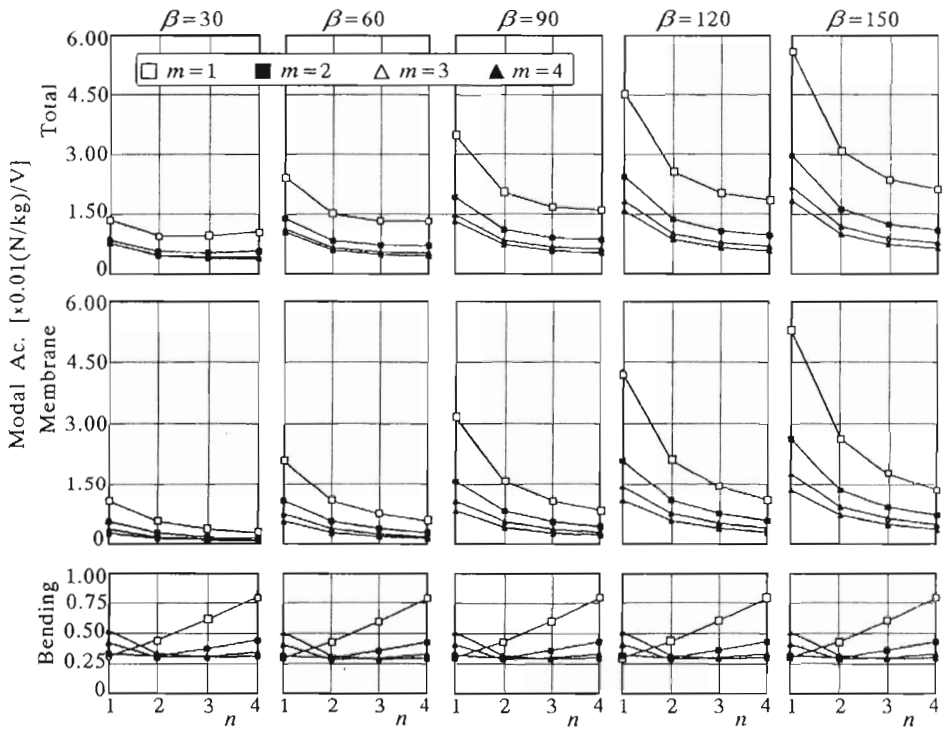

Fig. 6. Distributed control characteristics of shallow and deep shells

5.3. Distributed feedback characteristics

There are two sensor signal components (the membrane and bending components) and two actuation factors (the membrane and bending components). Thus, there are four possibilities: membrane signal to the membrane control (M,M); membrane signal to the bending control (M,B); bending signal to the membrane control (B,M), and bending signal to the bending control (M,M)

in the feedback control of the shells of curvatures of 30°, 60°, 90°, 120°, and 150°. Fig.7 illustrates the four feedback possibilities for the first nine natural modes of the shells. There are (M,M), (M,B), (B,M), (B,B) and the total effects plotted versus to the curvature angles, 30°, 60°, 90°, 120°, and 150° for the nine natural modes. It is clear that the (M,B) and (B,M) are symmetrical, thus they cancel out each other in the total response. However, the membrane effect increases as the curvature increases; the bending effect only changes slightly.

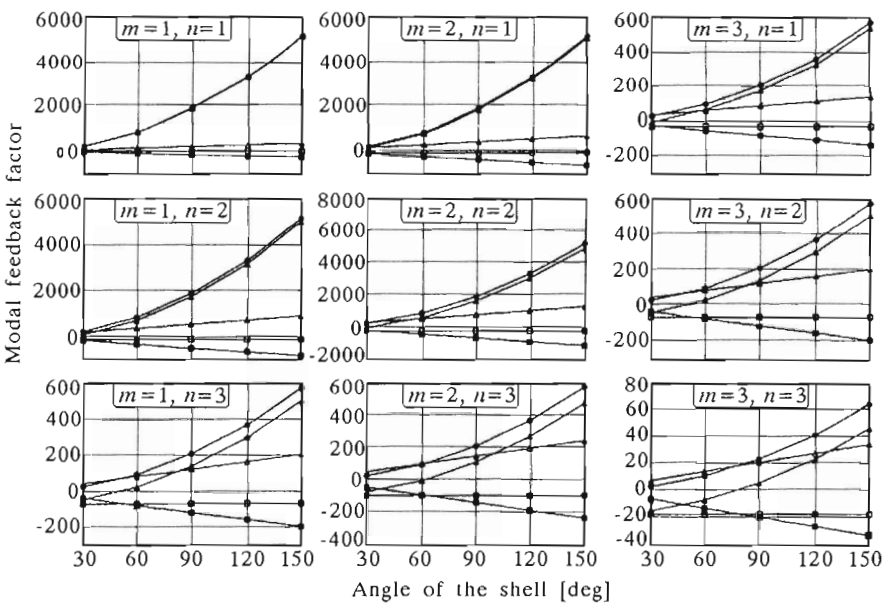

Fig. 7. Distributed feedback control characteristics of the shells; (M,M) • modal feedback factor from membrane sensor to membrane actuator; (B,B) □ modal feedback from bending sensor to bending actuator; (M,B) △ modal feedback factor from membrane sensor to bending actuator; (B,M) ■ modal feedback factor from bending sensor to membrane actuator; ▲ modal feedback factor of the controlled system

Again, it is clear that the membrane control effect dominates the overall control effect in deep shells, if the membrane signal can be individually extracted and fedback to the membrane actuators. The control effect resulting from the bending signal and the bending control effect (B,B) is relatively insignificant in lower natural modes of deep shells. Furthermore, damping variations of these four cases are also studied and plotted in Fig.8. These controlled damping characteristics also reveal similar characteristics as those discussed above.

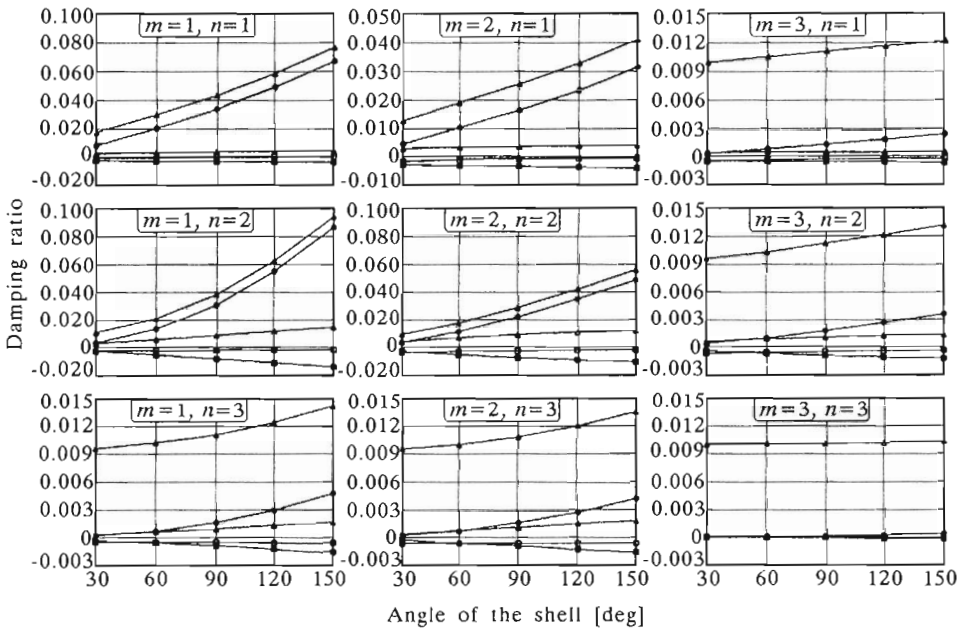

Fig. 8. Controlled damping characteristics of the shells; (M,M) • controlled damping ratio from membrane sensor to membrane actuator; (B,B) □ controlled damping ratio from bending sensor to bending actuator; (M,B) Δ controlled damping ratio from membrane sensor to bending actuator; (B,M) ■ controlled damping ratio from bending sensor to membrane actuator; ▲ damping ratio of the controlled system

6. Conclusions

Smart structures and structronic systems often involve multi-field coupling of structures, control, electronics, temperature, and applications of controllable smart materials, e.g., piezoelectrics, shape memory materials, electro- and magneto-strictive materials, electro- and magneto-rheological fluids, etc. The multi-field coupling and interactions of smart structures and structronic systems have revealed many complicated research issues in recent years. This paper presents an advanced nonlinear piezo(electric)-thermoelastic shell theory and a detailed analysis of electromechanical coupling of distributed piezoelectric sensors and actuators laminated on shell structures of various curvatures.

It was assumed that the flexible shells encounter the von Karman type large-deformation geometrical nonlinearity. Generic nonlinear electromechanical equations of piezo-thermoelastic shells and shell composites were derived using Hamilton's principle. Force and moment resultants for the piezo-

thermoelastic shell and the shell composite were defined, respectively; physical significance and control application of these terms were also discussed. As to investigate the distributed sensing and control characteristics, a set of shells with various curvatures was studied. Analytical results suggest that the total sensing/control effectiveness depends on individual contribution of the bending and the membrane components. The membrane component dominates the sensing/control effectiveness of lower natural modes of deep shells; the bending component dominates the sensing/control behavior of shallow shells and higher modes of deep shells. Feeding the membrane signal component to the membrane control maximizes the control effect in deep shells. However, applying the bending sensing component to the bending control maximizes the control effect in shallow and zero-curvature shells.

Acknowlwdgement

This research was supported, in part, by the Ford Research Laboratory.

References

1. CHAU L.K., 1986, The Theory of Piezoelectric Shells, *PMM USSR*, **50**, 1, 98-105

2. CHIA C.Y., 1980, *Nonlinear Analysis of Plates*, McGraw-Hill International Book Co., New York

3. DÖKMECI M.C., 1983, Dynamic Applications of Piezoelectric Crystals, *The Shock and Vibration Digest*, **15**, 3, 9-22

4. DRUMHELLER D.S., KALNINS A., 1970, Dynamic Shell Theroy for Ferroelectric Ceramics, *J. Acoust. Soc. Am.*, **47**, 5, 1343-1349

5. KOPPE H., GABBERT U., TZOU H.S., 1998, On Three-Dimensional Layered Piezoelectric Shell Elements for Design Simluation of Adaptive Structures, *Fortschritt-Berichte VDI, Smart Mechanical Systems - Adaptronics*, **13**, 125-136

6. LIBRESCU L., 1987, Refined Geometrically Nonlinear Theories of Anisotropic Laminated Shells, *Quarterly of Applied Mathematics*, **XLV**, 1, 1-22

7. MINDLIN R.D., 1972, High Frequency Vibrations of Piezoelectric Crystal Plates, *Inl. J. Solid Struc.*, **8**, 895-906

8. PAI P.F., NAFEH A.H., OH K., MOOK D.T., 1993, A Refined Nonlinear Model of Piezoelectric Plate, *J. Solids and Structures*, **30**, 1603-1630

9. PALAZOTTO A.N., DENNIS S.T., 1992, *Nonlinear Analysis of Shell Structures*, AIAA Pub., Washington, D.C.

10. PIETRASZKIEWICZ W., 1979, *Finite Rotations and Lagrangean Description in the Non-Linear Theory of Shells*, Polish Academy of Science, Polish Scientific Publishers

11. ROGACHEVA N.N., 1994, *The Theory of Piezoelectric Shells and Plates*, CRC Press, Boca Raton, FL

12. SENIK N.A., KUDRIAVTSEV B.A., 1980, Equations on the Theory of Piezoceramic Shells, In: *Mechanics of a Solid Deformable Body and Related Analytical Problems*. Moscow, Izd. mosk. Inst. Chim. Mashinostroeniia, USSR

13. TZOU H.S., 1998, Multi-Field Transducers, Devices, Mechatronic Systems and Structronic Systems with Smart Materials, *Shock and Vibration Digest*, **30**, 4, 282-294

14. TZOU H.S., 1993, *Piezoelectric Shells, Distributed Sensing and Control of Continua*, Kluwer Academic Pub. Dordrecht/Boston

15. TZOU H.S., BAO Y., 1997, Nonlinear Piezothermoelasticity and Multi-Field Actuations, Part-1: Nonlinear Anisotropic Piezothermoelastic Shell Laminates, *Journal of Vibration and Acoustics*, **119**, 374-381

16. TZOU H.S., BAO Y., VENKAYYA V.B., 1996, Study of Segmented Transducers Laminated on Cylindrical Shells, Part-1: Sensor Patches, and Part-2: Actuator Patches, *Journal of Sound and Vibration*, **197**, 2, 207-249

17. TZOU H.S., BERGMAN L.A., (Editors), 1998, *Dynamics and Control of Distributed Systems*, Cambridge University Press, New York, NY

18. TZOU H.S., GADRE M., 1989, Theoretical Analysis of a Multi-Layer Thin Shell Coupled with Piezoelectric Shell Actuators for Distributed Vibration Control, *Journal of Sound and Vibration*, **132**, 3, 433-450

19. TZOU H.S., HOWARD R.V., 1994, A Piezothermoelastic Thin Shell Theory Applied to Active Structures, *ASME Transactions, Journal of Vibration and Acoustics*, **116**, 3, 295-302

20. TZOU H.S., JOHNSON D., LIU JACK, 1999, Damping Behavior of Cantilever Structronic Systems with Boundary Control, *ASME Transactions, Journal of Vibration and Acoustics*, 402-407

21. TZOU H.S., YE R., 1994, Piezothermoelasticity and Precision Control of Piezoelectric Systems: Theory and Finite Element Analysis, *ASME Transactions, Journal of Vibration and Acoustics*, **116**, 4, 489-495

22. TZOU H.S., ZHONG J.P., HOLLKAMP J.J., 1994, Spatially Distributed Orthogonal Piezoelectric Shell Actuators: Theory and Applications, *Journal of Sound Vibration*, **177**, 3, 363-378

23. TZOU H.S., ZHONG J.P., NATORI M.C., 1993, Sensor Mechanics of Distributed Shell Convolving Sensors Applied to Flexible Rings, *ASME Transactions, Journal of Vibration and Acoustics*, **115**, 1, 40-46

24. TZOU H.S., ZHOU Y-H., 1995, Dynamics and Control of Nonlinear Circular Plates with Piezoelectric Actuators, *J. of Sound and Vibration*, **188**, 2, 189-207

Zastosowanie nieliniowej piezo-termosprężystej teorii powłok do sterowania powłok o zmiennej geometrii

Streszczenie

W pracy przedstawiono zastosowanie ogólnej nieliniowej piezo-termo-elektromechanicznej teorii do piezoelektrycznych powłok o podwójnej krzywiźnie oraz czteroparametrowego kontinuum niepowłokowego. Szczegółowo zbadano elektromechaniczne charakterystyki rozłożonego układu pomiarowego i wykonawczego w ciągu powłok o różnej geometrii. Wyniki wskazują, że membranowe elementy pomiarowe i wykonawcze panują nad dynamiką niskich częstości głębokoch powłok, a giętne elementy pomiarowe i wykonawcze nadają się do sterowania powłok małowyniosłych. Zbadano elektromechaniczne charakterystyki i efektywność rozłożonych elementów pomiarowych i wykonawczych.

Manuscript received January 3, 2000; accepted for print April 14, 2000